ELSEVIER

Contents lists available at ScienceDirect

Sensors and Actuators: B. Chemical

journal homepage: www.elsevier.com/locate/snb





Direct comparison of triggering motifs on chemiluminescent probes for hydrogen sulfide detection in water

Carolyn M. Levinn, Michael D. Pluth *

Department of Chemistry and Biochemistry, Materials Science Institute, Knight Campus for Accelerating Scientific Impact, Institute of Molecular Biology, University of Oregon, Eugene, Oregon, 97403, United States

ARTICLE INFO

Keywords: Hydrogen sulfide Chemiluminescence Detection Probe design

ABSTRACT

Hydrogen sulfide (H_2S) is an important biomolecule and significant efforts have focused on developing chemical tools to aid different biological investigations. Of such tools, there are relatively few chemiluminescent or bioluminescent methods for H_2S detection. Here we report two dioxetane-based chemiluminescent probes for H_2S detection. With these probes, we directly compare the probe response to H_2S -mediated azide reduction and nucleophilic displacement of 2,4-dinitrophenyl (DNP) motifs and demonstrate that the S_NA r cleavage of the DNP group results in a larger response and greater stability in water.

1. Introduction

Hydrogen sulfide (H2S) is the third recognized gasotransmitter and an important endogenously-produced biomolecule, [1,2] with roles in cardioprotection [3], neuroprotection [4], wound healing [5,6], and mitigating oxidative stress and associated damage [7,8]. For example, H₂S-producing enzymes are overexpressed in diabetic rats models and subsequent inhibition of enzymatic H2S production reduces hyperglycemia [9]. Conversely, in rat models of Parkinson's disease (PD), brain H₂S levels are significantly lower than in healthy control animals, and treatment with exogenous NaSH reverses the progression of PD symptoms [10-12]. Motivated by the growing and diverse roles of H₂S in different biological systems, the last decade has witnessed significant development of chemical tools for detection and delivery of H2S and related reactive sulfur species. Of such species, particular attention has focused on the development and expansion of biocompatible methods for H2S detection and quantification, with activity-based fluorescent probes providing useful platforms for visualizing H2S accumulation in cell culture and more complex experiments [13-17].

In parallel to fluorescent probe development, chemiluminescent probes for H_2S have also been developed, which provide an alternative approach for biological imaging that often results in lower background signal and greater tissue penetration due to the lack of excitation requirements [18,19]. Because chemiluminescent and bioluminescent platforms utilize a chemical reaction to generate an excited state intermediate, which emits photons upon relaxation back to ground state,

such systems typically result in reduced autofluorescence, photobleaching and phototoxicity, and background interference [20]. These favorable properties have led to the wide adoption of such probes as important tools for bioimaging and biochemical studies [21-24]. Demonstrating the diversity of this approach, prior probes have been developed for a wide array of small biomolecules, including hydrogen peroxide [25], singlet oxygen [26], formaldehyde [27], nitroxyl [28], as well as other analytes. For H2S detection, there are relatively few chemiluminescent or bioluminescent methods when compared to the number of available fluorescent probes. The first report of chemiluminescent H₂S detection was described by our group in 2013, in which H₂S-mediated azide reduction was used to convert azidoluminol to luminol [29,30]. Bioluminescent H₂S probes based on caged-luciferin were first reported by Lu and Li in 2015 and also leveraged H2S-mediated azide reduction [31,32]. In 2014, the first chemiluminescent H₂S probe based on Schaap's dioxetane [33] was reported by Sozmen and coworkers, which utilized the H₂S-responsive 2,4-dinitrophenol (DNP) based S_NAr trigger [34]. Schaap's dioxetane employs spiro-adamantyl dioxetanes, and the rigidity of this structure imparts enhanced thermal stability to the dioxetane [35]. This probe, however, required harsh basic conditions (pH 12) to generate a chemiluminescence response, which limits the potential utility for biological applications [34]. The Lippert group reported a dioxetane-based chemiluminescent H₂S probe in 2015, which utilized H₂S-mediated azide reduction to initiate a 1, 6-self-immolative elimination to reveal the luminogenic phenoxide [36]. These probes displayed moderate chemiluminescence under

E-mail address: pluth@uoregon.edu (M.D. Pluth).

^{*} Corresponding author.

biologically relevant conditions, however the response could be enhanced and red-shifted by the addition of 20% of the surfactant-dye adduct Emerald II Enhancer (Fig. 1a) [37]. Motivated by the scarcity of chemiluminescent probes for H_2S detection and lack of evaluation of H_2S -mediated modes of activation, we report here the preparation and direct comparison of two bright chemiluminescent probes for H_2S and evaluate their efficacy in aqueous solution with the goal of streamlining access to these useful chemical tools for H_2S -related investigations (Fig. 1b).

2. Results and discussion

To compare the efficacy of different H₂S sensing strategies, we chose to use the bright chemiluminescent dioxetane scaffold recently reported by the Shabat lab [38]. This luminophore, which is functionalized with a slightly deactivating chloride and an extended electron-withdrawing group para to the dioxetane, is $\sim 10^3$ -fold brighter than previously prepared similar cores. The additional electron-withdrawing groups and extended conjugation on the aromatic luminophore core red-shift the emission wavelength of this dioxetane probe by 55 nm when compared to the unfunctionalized phenol core [37,39,40]. Although H₂S-mediated azide reduction is the most common approach to H₂S detection, the rate of this reaction is significantly slower than S_NAr-based methods [41]. Based on these considerations, our goal was to compare the rate and efficacy of the H₂S-responsive azide system with the 2,4-dinitrophenol (DNP) electrophilic system, which undergo H₂S-mediated reduction to the parent amine and nucleophilic aromatic substitution, respectively (Fig. 2a). An additional key distinction between these systems is that the S_NAr electrophiles only require one equivalent of H₂S to initiate luminescence, [42] whereas azide reduction requires two equivalents of H₂S. Moreover, azide reduction results in H2S oxidation to generate polysulfides, which are biologically-relevant reactive sulfur species [43]. The mechanisms of activation of both the DNP cleavage and azide reduction by H2S have been reported previously, with examples provided in the references above. In addition, the 4-azido benzyl carbonate used to trigger self-immolation results in release of a para imino-quinone methide, which could potentially react with nucleophiles, although is likely scavenged by water to generate the corresponding benzyl alcohol.

To prepare these chemiluminescent probes, we reacted $\rm H_2S$ -responsive motifs with the previously-reported enol-ether phenol core $\rm EE-OH$, [38] followed by singlet oxygen oxidation (Fig. 2b). We initially used the Acid Red/Rose Bengal photosensitizer system for the generation of singlet oxidation, which has been used previously in the presence of azides, [36] but in our hands were unable to access clean alkene oxidation without azide photoreduction. We found, however, that using tetraphenyl porphyrin (TPP) [44] as the photosensitizer allowed for the reaction to be run in $\rm CH_2Cl_2$, which slows the decay of the generated singlet oxygen, reduces the reaction time, and decreases the amount of azide photodegredation [45]. These same photooxidation conditions were also used to prepare CL-DNP. We note that the final DNP product is significantly less photosensitive than CL-N3, which enabled greater scalability and a 76% yield over two steps compared to the 16% yield for the azide system.

With the two target probes in hand, we next measured the chemiluminescent response from the reaction of **CL-N3** and **CL-DNP** with H₂S. To simplify our initial investigations, we first measured the response in organic solution to eliminate potential complications with solubility, aggregation, or quenching in water. Our expectation was that the rate difference between CL-N3 and CL-DNP would be smaller in organic solvents due to prior reports demonstrating the enhanced rate of H2Smediated azide reduction in organic solution, when compared to aqueous systems [43]. Upon treatment of a 25 μM solution each probe with 100 equivalents of NaSH in THF we observed a significant increase in luminescence. Over the course of 30 min, the CL-N3 probe resulted in a luminescence turn on of over 2600-fold, which was much larger than the approximately 1450-fold luminescence turn on for CL-DNP (Fig. 3a, and SI). We attribute the difference in observed emission to the absorbance of 2,4-dinitrothiophenol (λ_{max} =450 nm) [46] generated from CL-DNP, which overlaps with the probe emission spectrum.

Having demonstrated that both the azide- and DNP-based probes function in THF, we next investigated the chemiluminescent responses in buffered water. Upon addition of **CL-N3** to degassed PBS buffer, we were surprised to observe a moderate, but rapid, increase in luminescence prior to the addition of NaSH. This reproducible result suggests

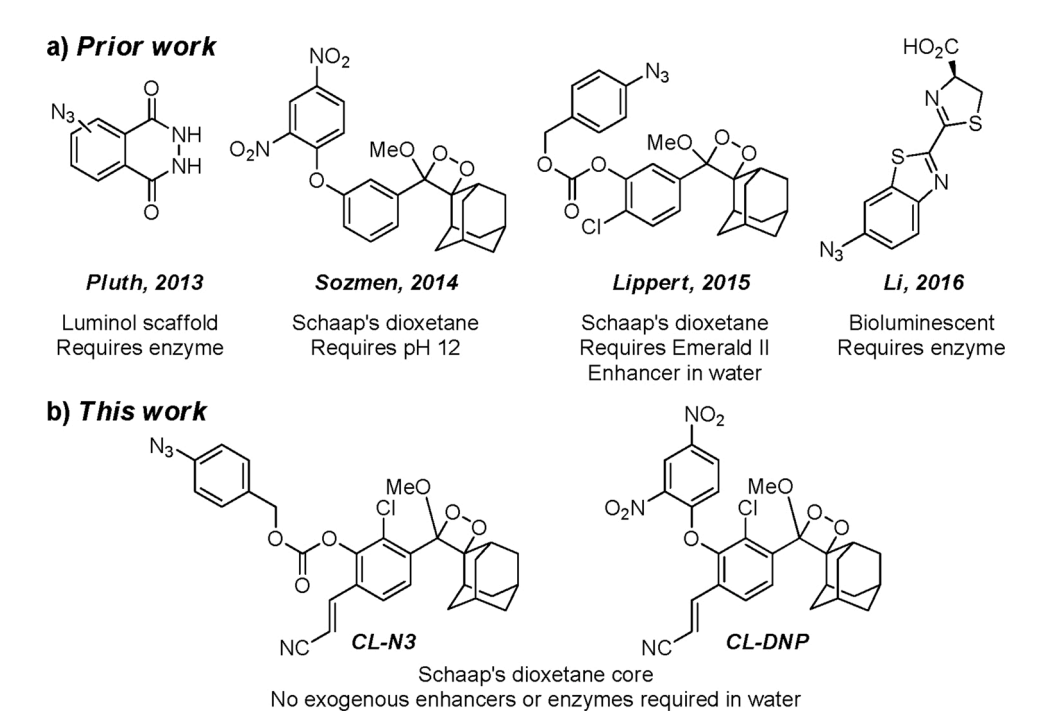


Fig. 1. a) Selected examples of prior chemiluminescent or bioluminescent H_2S probes. b) The two dioxetane-based chemiluminescent probes for H_2S with different triggering mechanisms used for direct comparison in this work.

Fig. 2. a) Mechanism and byproducts of H₂S-mediated turn-on of chemiluminescent probes CL-N3 and CL-DNP. b) Synthesis of the two probes CL-N3 and CL-DNP from the known phenol intermediate EE—OH.

that the triggering group on **CL-N3** may be unstable under aqueous conditions, possibly due to hydrolysis at the electrophilic carbonate. This observation limits the suitability of **CL-N3** probe for use in more complex biological imaging studies (Fig. 3b, inset). Due to the background turn on of **CL-N3** observed in buffer, the normalized turn-on response of **CL-N3** upon addition of 100 equiv. of NaSH over that of the background signal was only 7-fold. By contrast, the **CL-DNP** probe was found to be stable in PBS pH 7.4 buffer and resulted in a 100-fold increase in normalized luminescence after addition of 100 equiv. of NaSH (Fig. 3b). Importantly, this large change in luminescence does not require the addition of enhancers, unlike prior diooxetane-based H₂S probes.

Based on the greater stability of CL-DNP and significant luminescent response, we next carried out selectivity studies to confirm that the primary response is observed for H₂S. In these experiments, we treated **CL-DNP** with 100 equiv. of different analytes at 37 °C and measured the integrated luminescence response over 30 min. We chose to limit our selectivity investigations to specific biological nucleophiles due to the significant body of prior work in the literature focused on selectivity investigations. In general, these selectivity studies have demonstrated that primary competing analytes are biological nucleophiles, and little or no reactivity of the DNP group is observed with other potential biological reactants, including metal ions, reactive oxygen species, and reducing agents [47,48]. As expected, we observed a high selectivity for H₂S over the nucleophiles GSH, Cys, and Lys (Fig. 4a). For comparison, we have also included the integrated response in THF under identical conditions, which shows a significant increase in the overall luminescent signal. Notably, this probe does not require an enzyme activator nor an exogenous luminescence enhancer to function in aqueous environments. Moreover, the luminescent turn on of **CL-DNP** is significantly larger than previously-reported chemiluminescent or bioluminescent H₂S probes, as shown in Table 1.

In addition, we also measured the integrated chemiluminescent response to varying concentrations of $\rm H_2S$ in buffer over the range of 0–167 equiv. of NaSH over 30 min. At lower concentrations of NaSH, it is likely that the triggering $\rm S_NAr$ reaction may not by fully complete,

resulting in a lower integrated emission than expected. Nonetheless, a significant increase in luminescence is observed even when only 10 equiv. of NaSH are added to **CL-DNP**. Although the curvature of the chemiluminescence response precludes a definitive limit of detection, the chemiluminescence signal should be sufficient to detect relevant biological concentrations of $\rm H_2S$.

3. Conclusions

In summary, we prepared two bright chemiluminescent probes for $\rm H_2S$ detection that function without the need of brightness enhancers, surfactants, or enzyme activation. We demonstrated that in these systems, the more commonly used azide-trigger displayed moderate autoactivation in water, whereas the DNP-triggered probe was more stable. Moreover, the DNP-based system is significantly more synthetically accessible and shows good selectivity for $\rm H_2S$ over common biological nucleophiles. In a broader context, aryl azides can be reduced to the parent amine by the by cytochrome P450 enzymes, [49] whereas activation DNP groups by P450s has not been demonstrated to the best of our knowledge. These factors suggest that alternative approaches to the commonly used azide-reduction strategy may be more fruitful in biological settings.

4. Experimental section

4.1. Materials and methods

Reagents were purchased from Sigma-Aldrich, Tokyo Chemical Industry (TCI), Fisher Scientific, or VWR and used directly as received. Silica gel (SiliaFlash F60, Silicycle, 230 - 400 mesh) was used for column chromatography. Deuterated solvents were purchased from Cambridge Isotope Laboratories (Tewksbury, Massachusetts, USA). $^1\mathrm{H}$ and $^{13}\mathrm{C}\{^1\mathrm{H}\}$ NMR spectra were recorded on Bruker 500 MHz or Bruker 600 MHz NMR instruments at the indicated frequencies. Chemical shifts are reported in parts per million (δ) and are referenced to residual protic solvent resonances. The following abbreviations are used in describing

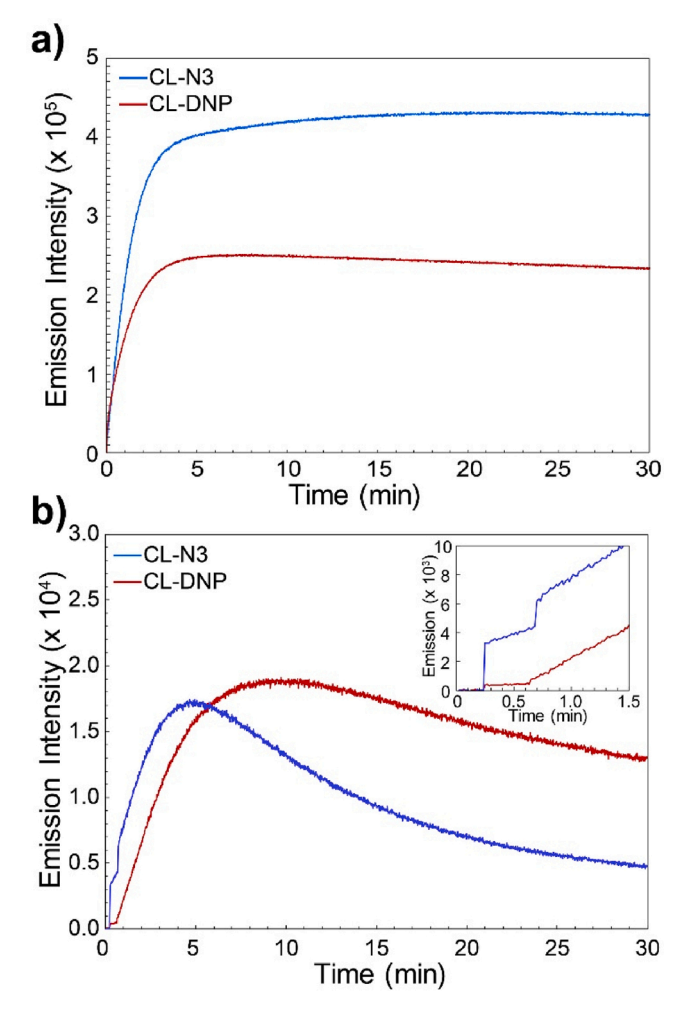


Fig. 3. a) Luminescent response of 25 μM solutions of CL-N3 and CL-DNP in THF to 100 equiv. of NaSH over 30 min at 37 °C. b) Luminescent response of 25 μM solutions of CL-N3 and CL-DNP in degassed 10 mM PBS 7.4 buffer with 5% DMSO to 100 equiv. of NaSH over 30 min at 37 °C. The inset shows the first 1.5 min of the experiment. The probe was added after about 20 s, and the NaSH was added after about 40 s.

NMR couplings: (s) singlet, (d) doublet, (b) broad, and (m) multiplet. IR spectra were measured on a Thermo Scientific Nicolet 6700 RT-IR using an ATR attachment. Mass spectrometric measurements were performed by the University of Illinois, Urbana Champaign MS facility. Phosphate buffered saline (PBS) tablets (1X, CalBioChem) were used to prepare buffered solutions (140 mM NaCl, 3.0 mM KCl, 10 mM phosphate, pH 7.4) in deionized water. Buffer solutions were sparged with nitrogen to remove dissolved oxygen and stored in an Innovative Atmosphere nitrogen-filled glovebox. All stock solutions were freshly prepared using degassed solvents immediately before use. Anhydrous sodium hydrogen sulfide (NaSH) was purchased from Strem Chemicals and handled under nitrogen. L-Cysteine and L-Lysine were purchased from TCI. Reduced glutathione was purchased from Aldrich. Stock solutions of the analytes were prepared in 10 mM PBS 7.4 buffer or DMSO under nitrogen immediately prior to use and were introduced into buffered solutions with an air-tight Hamilton syringe. Note: CL-N3 and CL-DNP are not air-sensitive, but protection of reaction solution from O₂ was to prevent H₂S oxidation. To ensure accurate measurements and to prevent decomposition of potentially reactive species, all experiments were performed under an inert atmosphere unless otherwise indicated. Chemiluminescence measurements were measured using a Quanta Master 40 spectrofluorometer (Photon Technology International) equipped with a Quantum Northwest TLC-50 temperature controller at

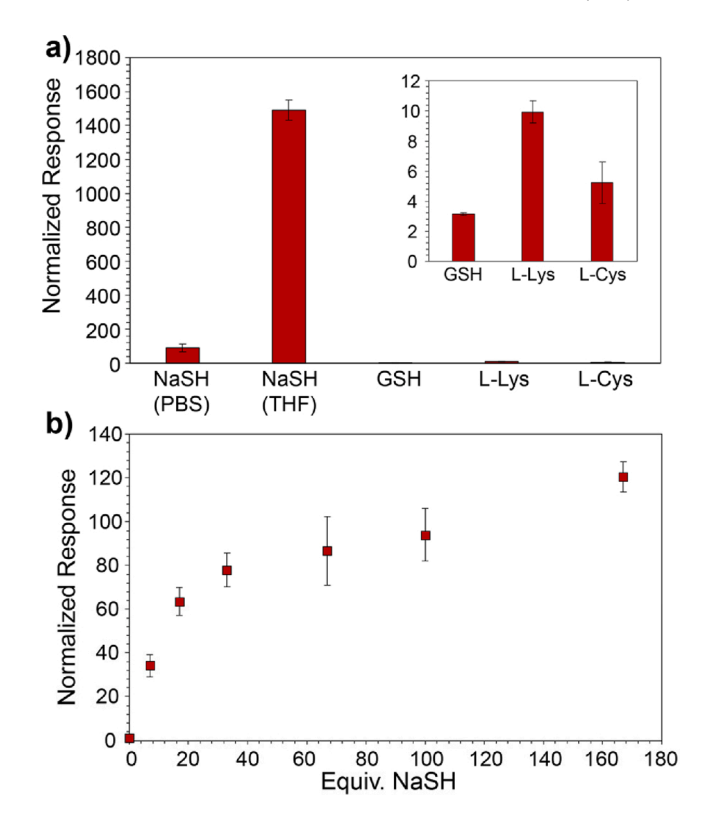


Fig. 4. a) Selectivity studies for **CL-DNP**. The THF data were acquired in airfree unstabilized THF and all other data were acquired in 10 mM degassed PBS 7.4 buffer with 5% DMSO. Each experiment was performed at 37 °C with 100 equiv. of NaSH and integrated over 30 min. Each bar represents the average normalized turn-on response of three independent trials relative to 25 μ M **CL-DNP** in PBS 7.4 buffer with 5% DMSO with no analyte added. b) Normalized chemiluminescent response of 25 μ M **CL-DNP** with increasing [NaSH]. NaSH experiments were performed in triplicate at 37 °C in 10 mM degassed PBS 7.4 buffer with 5% DMSO and integrated over 30 min.

Table 1Emission wavelengths and turn-on responses of **CL-DNP** and previously reported chemiluminescent and bioluminescent H₂S probes.

Probe	λ _{em} (nm)	Turn- on (fold)	Notes	Ref
CLSS-	425	45	50 µM probe, 33 equiv. H ₂ S, 5 min. integration, 37 °C, pH 7.4 Requires H ₂ O ₂ and horseradish peroxidase	Pluth 2013 [29]
Probe 6	475	0	100 μM probe, 10 equiv. H ₂ S. 25 °C, pH 12. No significant difference in signal with or without H ₂ S.	Sozmen 2014 [34]
CHS-3	545	7	$40 \mu M$ probe, 5 equiv. H_2S , 20 min. integration, 25 °C, pH 7.4 with 20% Emerald II Enhancer.	Lippert 2015 [36]
Probe 1	588	8	40 μ M probe, 250 equiv. H ₂ S, 60 min. integration, 37 °C, pH 7.4. Requires ATP and luciferase.	Li 2016 [31]
CL- DNP	525	100	$25~\mu M$ probe, 100 equiv. H_2S , 30 min. integration, $37~^{\circ}C$, pH 7.4 with 5% DMSO.	this work
		1600	$25~\mu\text{M}$ probe, 100 equiv. H_2S , 30 min. integration, $37~^{\circ}\text{C}$, THF.	

 37.0 ± 0.05 °C. All chemiluminescent measurements were made under an inert atmosphere in septum-sealed cuvettes obtained from Starna Scientific and were repeated at in triplicate.

4.2. Chemiluminescence studies

For all chemiluminescence experiments, excitation slits were closed, and the excitation wavelength were set to 800 nm. An excitation wavelength input was required for the instrument to acquire data, however this should not interfere with the measurement of chemiluminescent output. Emission slits were set to 4.0 mm, and the wavelength measured at was 525 nm. Scans were taken every second for at least 30 min. All experiments performed in triplicate.

4.2.1. General procedure in THF

In a septum sealed cuvette, 3.0 mL of degassed air-free THF was incubated for 5 min at 37 $^{\circ}\text{C}$, after which data collection was started. A 15 μL aliquot of the 5 mM THF stock solution of the probe was added using an airtight Hamilton syringe to make a 25 μM solution, then approximately 20 s later the desired analyte was added with an airtight Hamilton syringe. Data were collected for at least 30 min after the analyte was added.

4.2.2. General procedure in PBS

In a septum sealed cuvette, 3.0 mL of a solution of degassed 10 mM PBS 7.4 buffer with 5% DMSO was incubated for 5 min at 37 °C, after which data collection was started. A 15 μL aliquot of the 5 mM THF stock solution of the probe was added using an airtight Hamilton syringe to make a 25 μM solution, then approximately 20 s later the desired analyte was added with an airtight Hamilton syringe. Data were collected for at least 30 min after the analyte was added.

4.2.3. Preparation of stock solutions

In small HPLC vials, 500 mM NaSH, L-Cys, and L-Lys stock solutions were prepared in degassed Millipore water, and 15 μL were added for 100 equiv. experiments. Due to poor solubility, 250 mM GSH stock solutions were prepared in degassed Millipore water, and 30 μL of the GSH solution was added to the cuvette to reach 100 equiv. For the variable concentration NaSH experiments, the aliquots added were 0, 1, 2.5, 5, 10, 15, and 25 μL , to reach 0, 7, 17, 33, 67, 100, and 167 equivalents, respectively.

4.3. Normalized turn-on response

Data for four blank baseline response trials were collected with 25 μM of either CL-DNP or CL-N3 in either THF or PBS 7.4 with 5% DMSO at 37 $^{\circ} C$ for 30 min, with no analyte added. Identical fluorimeter parameters were used for each experiment: the excitation slits were closed, and the excitation wavelength set to 800 nm. Emission slits were set to 4.0 mm, and the wavelength measured was 525 nm. Scans were taken every second for at least 30 min. Background luminescence measurements were recorded and subtracted from all experiments when calculating the normalized luminescence response. The tabulated baseline responses are listed in Table S1.

4.4. Syntheses

CL-DNP. Core phenol **EE—OH** was prepared according to the literature procedures. Spectral data agrees with those reported in the literature [38,50]. **EE—OH** (100 mg, 0.281 mmol, 1.0 equiv.), 2, 4-dinitrobromobenzene (76 mg, 0.31 mmol, 1.1 equiv.) and K_2CO_3 (78 mg, 0.56 mmol, 2.0 equiv.) were dissolved in dry DMF (3 mL) and stirred overnight under N_2 . The reaction mixture was quenched with brine and extracted with EtOAc (3 \times 10 mL). The combined organic layers were washed with 5% aqueous LiCl (4 \times 10 mL), dried over anhydrous MgSO₄, concentrated under vacuum, and purified by silica column chromatography to yield 113 mg of a white solid. The crude DNP-enol ether product (110 mg, 0.211 mmol, 1.0 equiv.) was dissolved in CH₂Cl₂ (40 mL) and transferred to a large test tube. TPP (10 mg, 0.016 mmol, 0.05 equiv.) was added and mixed. The reaction tube was

clamped with the bottom 2 in. in an ice water bath and a steady stream of O2 was bubbled through a 9-inch Pasteur pipette into the solution while the reaction mixture was illuminated with a flood lamp. The reaction was run for three hours and with more CH2Cl2 was added every 20 min to maintain an approximately constant volume. The reaction was monitored by removing aliquots and measuring the ¹H NMR spectrum. After completion of the reaction, the crude reaction mixture was concentrated and purified by preparatory TLC (1:1 Hex:EtOAc, 1000 µm thick silica) to yield CL-DNP as a white solid (110 mg, 76 % yield over two steps). ¹H NMR (600 MHz, CDCl₃) δ (ppm): 8.93 (d, J = 2.73 Hz, 1 H), 8.28 (bs, 1 H), 8.23 (d, J = 8.49 Hz, 1 H), 7.73 (d, J = 8.49 Hz, 1 H), 7.47 (d, J = 16.72 Hz, 1 H), 6.48 (bs, 1 H), 6.19 (d, J = 16.72 Hz, 1 H), 3.19 (s, 3 H), 2.99 (s, 1 H), 2.09 (d, J = 13.31 Hz, 1 H), 1.93 (bs, 1 H), 1.83 (d, J = 13.31 Hz, 2 H), 1.76 - 1.56 (m, 7 H), 1.48 (dd, J = 13.05, 2.97 Hz, 1 H), 1.40 (d, J = 12.98 Hz, 1 H), 1.17 (d, J = 13.05 Hz, 1 H). 13 C{ 1 H} NMR (151 MHz, CDCl₃) δ (ppm): 153.97, 147.20, 142.23, 141.84, 138.63, 137.68, 131.99, 130.20, 129.02, 127.08, 125.76, 122.83, 116.81, 115.43, 111.15, 102.94, 96.32, 49.86, 36.30, 33.85, 33.67, 32.65, 32.02, 31.55, 31.49, 26.00, 25.67. IR (cm⁻¹) 2916.7, 2859.4, 2222.0, 1736.4, 1610.0, 1537.6, 1392.5, 1346.2, 1266.3, 1227.4, 1217.3, 1068.9. HRMS m/z [M + Na]⁺ calcd. for $[C_{27}H_{24}N_3O_8ClNa]^+$ 576.1150, found 576.1151.

CL-DNP. EE-OH (100 mg, 0.281 mmol, 1.0 equiv.), 2,4-dinitrobromobenzene (76 mg, 0.31 mmol, 1.1 equiv.), and K2CO3 (78 mg, 0.56 mmol, 2.0 equiv.) were dissolved in dry DMF (3 mL) and stirred overnight under N2. The reaction mixture was quenched with brine and extracted with EtOAc (3 imes 10 mL). The combined organic layers were washed with 5% aqueous LiCl (4 × 10 mL), dried over anhydrous MgSO₄, concentrated under vacuum, and purified by silica column chromatography to yield 113 mg of a white solid. The crude DNP-enol ether product (110 mg, 0.211 mmol, 1.0 equiv.) was dissolved in CH₂Cl₂ (40 mL) and transferred to a large test tube. TPP (10 mg, 0.016 mmol, 0.05 equiv.) was added and mixed. The reaction tube was clamped with the bottom 2 in. in an ice water bath, and a steady stream of O2 was bubbled through a 9-inch Pasteur pipette into the solution while the reaction mixture was illuminated with a flood lamp. The reaction was run for three hours and more CH2Cl2 was added every 20 min to maintain an approximately constant volume. The reaction was monitored by removing aliquots and measuring the ¹H NMR spectrum. After completion of the reaction, the crude reaction mixture was concentrated and purified by preparatory TLC (1:1 Hex:EtOAc, 1000 µm thick silica) to yield **CL-DNP** as a white solid (110 mg, 76% yield over two steps). ¹H NMR (600 MHz, CDCl₃) δ (ppm): 8.93 (d, J = 2.73 Hz, 1 H), 8.28 (bs, 1 H), 8.23 (d, J = 8.49 Hz, 1 H), 7.73 (d, J = 8.49 Hz, 1 H), 7.47 (d, J = 16.72 Hz, 1 H), 6.48 (bs, 1 H), 6.19 (d, J = 16.72 Hz, 1 H), 3.19 (s, 3 H), 2.99 (s, 1 H), 2.09 (d, J = 13.31 Hz, 1 H), 1.93 (bs, 1 H), 1.83 (d, J = 13.31 Hz, 2 H), 1.76–1.56 (m, 7 H), 1.48 (dd, J = 13.05, 2.97 Hz, 1 H), 1.40 (d, J = 12.98 Hz, 1 H), 1.17 (d, J = 13.05 Hz, 1 H). ¹³C{¹H} NMR (151 MHz, CDCl₃) δ (ppm): 153.97, 147.20, 142.23, 141.84, 138.63, 137.68, 131.99, 130.20, 129.02, 127.08, 125.76, 122.83, 116.81, 115.43, 111.15, 102.94, 96.32, 49.86, 36.30, 33.85, 33.67, 32.65, 32.02, 31.55, 31.49, 26.00, 25.67. IR (cm⁻¹) 2916.7, 2859.4, 2222.0, 1736.4, 1610.0, 1537.6, 1392.5, 1346.2, 1266.3, 1227.4, 1217.3, 1068.9. HRMS m/z [M + Na]⁺ calcd. for [C₂₇H₂₄N₃O₈ClNa]⁺ 576.1150, **CL-N3**. **EE**-**OH** (515 mg, 1.45 mmol, 1.2 equiv.) and the azide carbonate coupling partner (350 mg, 1.21 mmol, 1.0 equiv.)³⁶ were dissolved in 20 mL of 4:1 THF:CH₂Cl₂ under N₂. DMAP (221 mg, 1.81 mmol, 1.5 equiv.) and Et₃N (0.67 mL, 4.83 mmol, 4.0 equiv.) were added, and the resultant reaction mixture was stirred overnight protected from light. The reaction mixture was quenched with brine and extracted with EtOAc (3 \times 20 mL). The combined organic layers were dried over anhydrous MgSO₄, concentrated under vacuum, and purified by preparatory TLC (1:1 Hex:EtOAc, 1000 μm silica thickness). The resulting N3-enol ether (120 mg, 0.226 mmol, 1.0 equiv.) was then dissolved in CH2Cl2 (40 mL) and transferred to a large test tube. TPP (7 mg, 0.01 mmol, 0.05 equiv.) was added and

mixed. The reaction tube was clamped with the bottom 2 in. in an ice water bath, and a steady stream of O2 was bubbled through a 9-inch Pasteur pipette into the solution while the reaction mixture was illuminated with a flood lamp. The reaction was run for three hours and with more CH2Cl2 was added every 20 min to maintain an approximately constant volume. The reaction was monitored by removing aliquots and measuring the ¹H NMR spectrum. The crude reaction mixture was concentrated and purified by preparatory TLC (2:1 Hex:EtOAc, $1000 \ \mu m$ silica thickness) to yield CL-N3 as a white solid (87 mg 16%yield as a white solid) ¹H NMR (500 MHz, CDCl₃) δ (ppm): 8.08 (d, J =8.44 Hz, 1 H, 7.56 (d, J = 8.44 Hz, 1 H), 7.42 (m, 3 H), 7.07 (d, J = 8.48 Hz, 1 H)Hz, 2 H), 6.01 (d, J = 16.76 Hz, 1 H), 5.29 (s, 2 H), 3.19 (s, 3 H), 3.01 (bs, 1 H), 2.21 (d, J = 13.28 Hz, 1 H), 1.92 (bs, 1 H), 1.83 (m, 2 H), 1.73 (m, 4 H), 1.65 (m, 1 H), 1.59 (m, 2 H), 1.46 (dd, J = 12.92, 3.00 Hz, 1 H), 1.33 (dd, J = 13.48, 3.00 Hz, 1 H). ¹³C{¹H} NMR (126 MHz, CDCl₃) δ (ppm): 151.68, 146.16, 142.70, 141.10, 136.39, 131.06, 130.69, 130.34, 129.53, 127.42, 124.67, 119.40, 117.14, 111.35, 101.63, 96.39, 70.93, 49.81, 36.50, 33.90, 33.61, 32.41, 32.14, 31.56, 31.52, 26.11, 25.76. IR (cm⁻¹) 2910.9, 2858,4, 2221.32, 2110.0, 1767.4, 1508.4, 1453.1, 1397.9, 1376.5, 1210.7, 1180.2, 1128.8, 1104.6, 1068.6. HRMS m/z [M + Na]⁺ calcd. for $[C_{29}H_{27}N_4O_6ClNa]^+$ 585.1517, found 585.1529. found 576.1151.

Supporting information

 $^{1}\mathrm{H}$ and $^{13}\mathrm{C}\{^{1}\mathrm{H}\}$ NMR spectra of new compounds, chemiluminescence data.

CRediT authorship contribution statement

Carolyn M. Levinn: Conceptualization, Investigation. Michael D. Pluth: Conceptualization, Supervision.

Declaration of Competing Interest

The authors report no declarations of interest.

Acknowledgements

This research was supported by the NIH (R01GM113030) and NSFGRFP (DGE-1309047). NMR instrumentation in the UO CAMCOR facility is supported by the NSF (CHE-1427987 and CHE-1625529).

Appendix A. Supplementary data

Supplementary material related to this article can be found, in the online version, at doi:https://doi.org/10.1016/j.snb.2020.129235.

References

- [1] R. Wang, Two's company, three's a crowd: Can H₂S be the third endogenous gaseous transmitter? Faseb J. 16 (2002) 1792–1798, https://doi.org/10.1096/fi.02-0211hyp.
- [2] M.R. Filipovic, J. Zivanovic, B. Alvarez, R. Banerjee, Chemical biology of H₂S signaling through Persulfidation, Chem. Rev. 118 (2018) 377–461, https://doi.org/10.1021/acs.chemrev.7b00205.
- [3] M. Lavu, S. Bhushan, D.J. Lefer, Hydrogen sulfide-mediated cardioprotection: mechanisms and therapeutic potential, Clin. Sci. 120 (2011) 219–229, https://doi. org/10.1042/cs/20100462.
- [4] W.L. Chen, Y.Y. Niu, W.Z. Jiang, H.L. Tang, C. Zhang, Q.M. Xia, X.Q. Tang, Neuroprotective effects of hydrogen sulfide and the underlying signaling pathways, Rev. Neurosci. 26 (2015) 129–142. https://doi.org/10.1515/revneuro-2014-0051.
- [5] M.T. Xu, Y.Y. Hua, Y. Qi, G.L. Meng, S.J. Yang, Exogenous hydrogen sulphide supplement accelerates skin wound healing via oxidative stress inhibition and vascular endothelial growth factor enhancement, Exp. Dermatol. 28 (2019) 776–785. https://doi.org/10.1111/exql.13930
- [6] H.C. Zhao, S.X. Lu, J.H. Chai, Y.C. Zhang, X.L. Ma, J.C. Chen, Q.B. Guan, M.Y. Wan, Y.T. Liu, Hydrogen sulfide improves diabetic wound healing in Ob/Ob mice via attenuating inflammation, J. Diabetes Complicat. 31 (2017) 1363–1369, https://doi.org/10.1016/j.jdiacomp.2017.06.011.

- [7] S. Carballal, M. Trujillo, E. Cuevasanta, S. Bartesaghi, M.N. Moller, L.K. Folkes, M. A. Garcia-Bereguiain, C. Gutierrez-Merino, P. Wardman, A. Denicola, R. Radi, B. Alvarez, Reactivity of hydrogen sulfide with peroxynitrite and other oxidants of biological interest, Free Radic. Biol. Med. 50 (2011) 196–205, https://doi.org/10.1016/j.freeradbiomed.2010.10.705.
- [8] J.L. Wallace, R. Wang, Hydrogen sulfide-based therapeutics: exploiting a unique but ubiquitous gasotransmitter, Nat. Rev. Drug Discov. 14 (2015) 329–345, https://doi.org/10.1038/nrd4433.
- [9] L.Y. Wu, W. Yang, X.M. Jia, G.D. Yang, D. Duridanova, K. Cao, R. Wang, Pancreatic islet overproduction of H₂S and suppressed insulin release in zucker diabetic rats, Lab. Investig. 89 (2009) 59–67, https://doi.org/10.1038/labinvest.2008.109.
- [10] Q.H. Gong, X.R. Shi, Z.Y. Hong, L.L. Pan, X.H. Liu, Y.Z. Zhu, A new hope for neurodegeneration: possible role of hydrogen sulfide, J. Alzheimer Dis. 24 (2011) 173–182, https://doi.org/10.3233/jad-2011-110128.
- [11] L.F. Hu, M. Lu, C.X. Tiong, G.S. Dawe, G. Hu, J.S. Bian, Neuroprotective effects of hydrogen sulfide on Parkinson's disease rat models, Aging Cell 9 (2010) 135–146, https://doi.org/10.1111/j.1474-9726.2009.00543.x.
- [12] M. Sarukhani, H. Haghdoost-Yazdi, A.S. Golezari, A. Babayan-Tazehkand, T. Dargahi, N. Rastgoo, Evaluation of the antiparkinsonism and neuroprotective effects of hydrogen sulfide in acute 6-hydroxydopamine-Induced animal model of Parkinson's disease: behavioral, histological and biochemical studies, Neurol. Res. 40 (2018) 525–533, https://doi.org/10.1080/01616412.2017.1390903.
- [13] F.B. Yu, X.Y. Han, L.X. Chen, Fluorescent probes for hydrogen sulfide detection and bioimaging, Chem. Commun. 50 (2014) 12234–12249, https://doi.org/10.1039/ c4cc03312d
- [14] A.R. Lippert, Designing reaction-based fluorescent probes for selective hydrogen sulfide detection, J. Inorg. Biochem. 133 (2014) 136–142, https://doi.org/ 10.1016/j.jinorgbio.2013.10.010.
- [15] C.Y. Zhang, Q.Z. Zhang, K. Zhang, L.Y. Li, M.D. Pluth, L. Yi, Z. Xi, Dual-biomarker-Triggered fluorescence probes for differentiating cancer cells and revealing synergistic antioxidant effects under oxidative stress, Chem. Sci. 10 (2019) 1945–1952, https://doi.org/10.1039/c8sc03781g.
- [16] L.L. Zhang, H.K. Zhu, C.C. Zhao, X.F. Gu, A near-infrared fluorescent probe for monitoring fluvastatin-stimulated endogenous H₂S production, Chinese Chem. Lett. 28 (2017) 218–221, https://doi.org/10.1016/j.cclet.2016.07.008.
- [17] J.P. Wang, Y. Wen, F.J. Huo, C.X. Yin, Based' Successive' nucleophilic substitution mitochondrial-targeted H₂S red light emissive fluorescent probe and its imaging in mice, Sens. Actuators B-Chem. 297 (2019), 126773, https://doi.org/10.1016/j. spb.2019.126773.
- [18] M.A. Paley, J.A. Prescher, Bioluminescence: a versatile technique for imaging cellular and molecular features, Medchemcomm 5 (2014) 255–267, https://doi. org/10.1039/c3md00288h.
- [19] C.M. Rathbun, J.A. Prescher, Bioluminescent probes for imaging biology beyond the culture dish, Biochemistry 56 (2017) 5178–5184, https://doi.org/10.1021/acs. biochem.7b00435.
- [20] Y.C. Yan, P.F. Shi, W.L. Song, S. Bi, Chemiluminescence and bioluminescence imaging for biosensing and therapy: in vitro and in vivo perspectives, Theranostics 9 (2019) 4047–4065, https://doi.org/10.7150/thno.33228.
- [21] W.B. Porterfield, K.A. Jones, D.C. McCutcheon, J.A. Prescher, A "Caged" luciferin for imaging cell-Cell contacts, J. Am. Chem. Soc. 137 (2015) 8656–8659, https:// doi.org/10.1021/jacs.5b02774.
- [22] K. Suzuki, T. Nagai, Recent progress in expanding the chemiluminescent toolbox for bioimaging, Curr. Opin. Biotechnol. 48 (2017) 135–141, https://doi.org/ 10.1016/j.copbio.2017.04.001.
- [23] C.E. Badr, B.A. Tannous, Bioluminescence imaging: progress and applications, Trends Biotechnol. 29 (2011) 624–633, https://doi.org/10.1016/j. tibtech.2011.06.010.
- [24] N. Siraj, B. El-Zahab, S. Hamdan, T.E. Karam, L.H. Haber, M. Li, S.O. Fakayode, S. Das, B. Valle, R.M. Strongin, G. Patonay, H.O. Sintim, G.A. Baker, A. Powe, M. Lowry, J.O. Karolin, C.D. Geddes, I.M. Warner, Fluorescence, phosphorescence, and chemiluminescence, Anal. Chem. 88 (2016) 170–202, https://doi.org/ 10.1021/acs.analchem.5b04109.
- [25] D. Lee, S. Khaja, J.C. Velasquez-Castano, M. Dasari, C. Sun, J. Petros, W.R. Taylor, N. Murthy, In vivo imaging of hydrogen peroxide with chemiluminescent nanoparticles, Nat. Mater. 6 (2007) 765–769, https://doi.org/10.1038/nmat1983.
- [26] N. Hananya, O. Green, R. Blau, R. Satchi-Fainaro, D. Shabat, A highly efficient chemiluminescence probe for the detection of singlet oxygen in living cells, Angewandte Chemie-International Edition 56 (2017) 11793–11796, https://doi. org/10.1002/anie.201705803.
- [27] K.J. Bruemmer, O. Green, T.A. Su, D. Shabat, C.J. Chang, Chemiluminescent probes for activity-based sensing of formaldehyde released from folate degradation in living mice, Angewandte Chemie-Int. Edition 57 (2018) 7508–7512, https://doi. org/10.1002/anie.201802143.
- [28] W.W. An, L.S. Ryan, A.G. Reeves, K.J. Bruemmer, L. Mouhaffel, J.L. Gerberich, A. Winters, R.P. Mason, A.R. Lippert, A chemiluminescent probe for HNO quantification and real-time monitoring in living cells, Angewandte Chemie-Int. Edition 58 (2019) 1361–1365, https://doi.org/10.1002/anie.201811257.
- [29] T.S. Bailey, M.D. Pluth, Chemiluminescent detection of enzymatically produced hydrogen sulfide: substrate hydrogen bonding influences selectivity for H₂S over biological thiols, J. Am. Chem. Soc. 135 (2013) 16697–16704, https://doi.org/ 10.1021/jad08909h
- [30] T.S. Bailey, M.D. Pluth, in: E. Cadenas, L. Packer (Eds.), Chemiluminescent Detection of Enzymatically Produced H₂S. In Hydrogen Sulfide in Redox Biology, Pt A, 554, 2015, pp. 81–99.

- [31] B.W. Ke, W.X. Wu, W. Liu, H. Liang, D.Y. Gong, X.T. Hu, M.Y. Li, Bioluminescence probe for detecting hydrogen sulfide in vivo, Anal. Chem. 88 (2016) 592–595, https://doi.org/10.1021/acs.analchem.5b03636.
- [32] X.D. Tian, Z.Y. Li, C.W. Lau, J.Z. Lu, Visualization of in vivo hydrogen sulfide production by a bioluminescence probe in cancer cells and nude mice, Anal. Chem. 87 (2015) 11325–11331, https://doi.org/10.1021/acs.analchem.5b03712.
- [33] A.P. Schaap, M.D. Sandison, R.S. Handley, Chemical and enzymatic triggering of 1,2-Dioxetanes .3. Alkaline phosphatase-catalyzed chemiluminescence from an aryl phosphate-substituted dioxetane, Tetrahedron Lett. 28 (1987) 1159–1162, https://doi.org/10.1016/s0040-4039(00)95314-0.
- [34] I.S. Turan, F. Sozmen, A chromogenic dioxetane chemosensor for hydrogen sulfide and pH dependent off-on chemiluminescence property, Sens. Actuators B-Chem. 201 (2014) 13–18, https://doi.org/10.1016/j.snb.2014.04.101.
- [35] G.B. Schuster, N.J. Turro, H.C. Steinmetzer, A.P. Schaap, G. Faler, W. Adam, J. C. Liu, Adamantylideneadamantane-1,2-Dioxetane Investigation of chemiluminescence and decomposition kinetics of an unusually stable 1,2-Dioxetane, J. Am. Chem. Soc. 97 (1975) 7110–7118, https://doi.org/10.1021/ia00857a024
- [36] J. Cao, R. Lopez, J.M. Thacker, J.Y. Moon, C. Jiang, S.N.S. Morris, J.H. Bauer, P. Tao, R.P. Mason, A.R. Lippert, Chemiluminescent probes for imaging H₂S in living animals, Chem. Sci. 6 (2015) 1979–1985, https://doi.org/10.1039/ cdc002516i
- [37] S. Gnaim, O. Green, D. Shabat, The emergence of aqueous chemiluminescence: new promising class of phenoxy 1,2-dioxetane luminophores, Chem. Commun. 54 (2018) 2073–2085, https://doi.org/10.1039/c8cc00428e.
- [38] O. Green, T. Eilon, N. Hananya, S. Gutkin, C.R. Bauer, D. Shabat, Opening a gateway for chemiluminescence cell imaging: distinctive methodology for design of bright chemiluminescent dioxetane probes, ACS Cent. Sci. 3 (2017) 349–358, https://doi.org/10.1021/acscentsci.7b00058.
- [39] N. Hananya, D. Shabat, Recent advances and challenges in luminescent imaging: bright outlook for chemiluminescence of dioxetanes in water, ACS Cent. Sci. 5 (2019) 949–959, https://doi.org/10.1021/acscentsci.9b00372.
- [40] N. Hananya, J.P. Reid, O. Green, M.S. Sigman, D. Shabat, Rapid chemiexcitation of phenoxy-dioxetane luminophores yields ultrasensitive chemiluminescence assays, Chem. Sci. 10 (2019) 1380–1385, https://doi.org/10.1039/c8sc04280b.
- [41] L.A. Montoya, T.F. Pearce, R.J. Hansen, L.N. Zakharov, M.D. Pluth, Development of selective colorimetric probes for hydrogen sulfide based on nucleophilic aromatic substitution, J. Org. Chem. 78 (2013) 6550–6557, https://doi.org/10.1021/ io4008095
- [42] Z.J. Huang, S.S. Ding, D.H. Yu, F.H. Huang, G.D. Feng, Aldehyde group assisted thiolysis of dinitrophenyl ether: a new promising approach for efficient hydrogen sulfide probes, Chem. Commun. 50 (2014) 9185–9187, https://doi.org/10.1039/ c4c03818e.

- [43] H.A. Henthorn, M.D. Pluth, Mechanistic insights into the H₂S-Mediated reduction of aryl azides commonly used in H₂S detection, J. Am. Chem. Soc. 137 (2015) 15330–15336, https://doi.org/10.1021/jacs.5b10675.
- [44] T. Handa, H. Takeuchi, H. Takagi, S. Toriyama, Y. Kawashima, H. Komatsu, M. Nakagaki, Reactivity of singlet oxygen generated by the photosensitization of Tetraphenylporphyrin in liposomes, Colloid Polym. Sci. 266 (1988) 745–752, https://doi.org/10.1007/bf01410285.
- [45] G.P. Gurinovich, K.I. Salokhiddinov, I.M. Byteva, Lifetime of singlet oxygen in various solvents, J. Appl. Spectrosc. 34 (1981) 561–564.
- [46] W. Zhang, J.Q. Kang, P. Li, H. Wang, B. Tang, Dual signaling molecule sensor for rapid detection of hydrogen sulfide based on modified tetraphenylethylene, Anal. Chem. 87 (2015) 8964–8969, https://doi.org/10.1021/acs.analchem.5b02169.
- [47] X.W. Cao, W.Y. Lin, K.B. Zheng, L.W. He, A near-infrared fluorescent turn-on probe for fluorescence imaging of hydrogen sulfide in living cells based on thiolysis of dinitrophenyl ether, Chem. Commun. 48 (2012) 10529–10531, https://doi.org/ 10.1039/c2cc34031c.
- [48] V.S. Lin, W. Chen, M. Xian, C.J. Chang, Chemical probes for molecular imaging and detection of hydrogen sulfide and reactive sulfur species in biological systems, Chem. Soc. Rev. 44 (2015) 4596–4618, https://doi.org/10.1039/c4cs00298a.
- [49] L.J. O'Connor, I.N. Mistry, S.L. Collins, L.K. Folkes, G. Brown, S.J. Conway, E. M. Hammond, Cyp450 enzymes effect oxygen-dependent reduction of azide-based fluorogenic dyes, ACS Cent. Sci. 3 (2017) 20–30, https://doi.org/10.1021/acscentsci.6b00276.
- [50] N. Hananya, A.E. Boock, C.R. Bauer, R. Satchi-Fainaro, D. Shabat, Remarkable enhancement of chemiluminescent signal by dioxetane-fluorophore conjugates: turn-on chemiluminescence probes with color modulation for sensing and imaging, J. Am. Chem. Soc. 138 (2016) 13438–13446, https://doi.org/10.1021/jacs.6b09173.

Carolyn Levinn earned her B.S. in chemistry from the State University of New York (SUNY) College at Geneseo in 2014. She earned her M.S. in chemistry from the University of Illinois at Urbana–Champian in 2017. She is currently pursuing her Ph.D. in organic chemistry at the University of Oregon. Her research centers around the development of small molecule donors and probes for the detection and delivery of $\rm H_{2}S$ and COS.

Michael Pluth received his B.S. in chemistry and applied mathematics from the University of Oregon in 2004 and his PhD from UC Berkeley in 2008. He is currently a Professor in the Department of Chemistry & Biochemistry at the University of Oregon. His research interests are thematically based on different aspects of molecular recognition at the interface of bioorganic and bioinorganic chemistry. Much of his lab focuses on developing chemical tools for $\rm H_2S$ detection and quantification and using bioinorganic models to investigate the chemical mechanisms by which $\rm H_2S$ exerts action.